Polymer Chemistry

Accepted Manuscript

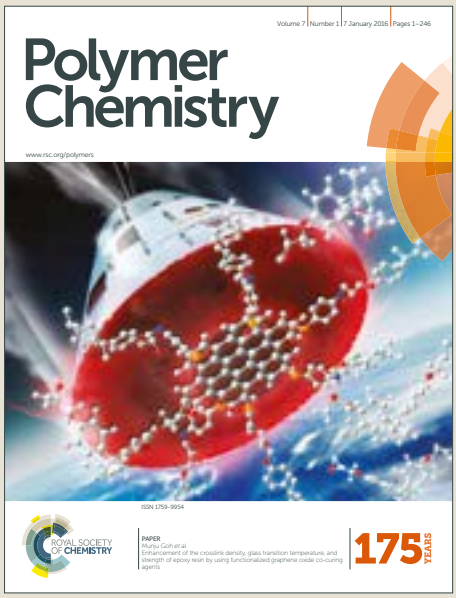

ROYAL SOCIETY OF CHEMISTRY

rsc.li/polymers

View Article Online
DOI: 10.1039/C8PY00600H

Crosslinked casein-based micelles as a dually responsive drug delivery system

Matias Luis Picchio,[1,2Ψ] Julio César Cuggino,[3Ψ] Gregor Nagel,[4] Stefanie Wedepohl,[4] Roque Javier Minari,[3] Cecilia Inés Alvarez Igarzabal,[1] Luis Marcelino Gugliotta[3]* and Marcelo Calderón[4]*

[1)] *Departamento de Química Orgánica, Facultad de Ciencias Químicas, Universidad Nacional de Córdoba (UNC), IPQA-CONICET, Haya de la Torre y Medina Allende. Ciudad Universitaria. Córdoba (5000) Argentina*

[2)] *GIDAIQ, Facultad Regional Villa María (Universidad Tecnológica Nacional), Av. Universidad 450, Villa María (5900) Argentina.*

[3)] *Polymer Reaction Engineering Group, INTEC (Universidad Nacional del Litoral-CONICET), Güemes 3450, Santa Fe 3000, Argentina*

[4)] *Freie Universität Berlin, Institut für Chemie und Biochemie, Takustrasse 3, 14195 Berlin, Germany*

[Ψ] These authors contributed equally to this work

*Corresponding authors:

Prof. Dr. Luis Marcelino Gugliotta

Instituto de Desarrollo Tecnológico para la Industria Química (INTEC), CONICET

Güemes 3450, 3000 Santa Fe, Argentina

TEL / FAX: (54) 342 455 9174/77

E-mail: lgug@intec.unl.edu.ar

Prof. Dr. Marcelo Calderón

Institut für Chemie und Biochemie, Freie Universität Berlin.

Takustrasse 3, 14195 Berlin, Germany

TEL / FAX: (49) 30 838 459368

E-mail: marcelo.calderon@fu-berlin.de

View Article Online
DOI: 10.1039/C8PY00600H

ABSTRACT

New types of biodegradable nanocarriers for drug delivery were prepared using casein (CAS) micelles as particle templates and glyceraldehyde (GAL) as a crosslinking agent. We found that highly crosslinked casein micelles (CCM) maintained their structural integrity at pH 7.4 (plasma conditions) but were easily degraded in the presence of proteases at pH 5 (lysosomal conditions). Nile red (NR) was chosen as a hydrophobic model drug inspired by the natural role of casein as lipophilic nutrient nanotransporter. The cumulative release of the NR-loaded micelles showed marginal dye leakage at pH 7.4 but was significantly accelerated by protease and pH–mediated degradation of the nanocarriers in a dual-responsive fashion. The prepared nanocarriers possess many favorable features for drug delivery: excellent biocompatibility and biodegradability, high stability in physiological conditions, remarkable capacity for the encapsulation of hydrophobic drugs, minimal drug leakage under extracellular conditions, and rapid drug release in response to the endo-lysosomal levels of pH and proteases. In this regard, the prepared CCM represent a promising candidate for the delivery and triggered release of anti-cancer drugs in lysosomal environments.

Keywords: protein carriers, casein micelles, drug delivery, nanocarriers, cancer therapy.

View Article Online
DOI: 10.1039/C8PY00600H

1. Introduction

Over the last years, the development of nanoparticles based on bio-polymers for application as drug delivery systems (DDS) has gained attention due to their intrinsic biocompatibility and biodegradability compared with nanoparticles based on synthetic polymers.[1–4] In particular, the preparation of protein-based nanocarriers for their utilization as DDS is an area of growing interest.[5–10] In addition to biodegradability and biocompatibility, proteins have an interesting variety of easily modifiable functional groups such as carboxylic acids (glutamic or aspartic acid), amines (lysine and arginine) and thiols (cysteine) in their primary structure. These groups provide a great variety of crosslinking points for network formation and stabilization,[11] polymer conjugation,[12,13] nanoparticle modification/functionalization with target molecules[14,15] or drug binding via chemical,[16] hydrophobic,[17] or ionic bonds[18] among others.

Casein (CAS) is a nutritive milk protein with excellent biocompatibility, biodegradability, and high abundance. These properties characterize CAS as an attractive bio-polymer for the development of novel, pharmaceutical materials.[19,20] The intrinsic property of CAS to form micelles in aqueous solution in the presence of Ca^{2+} ions offers a template for the formation of nanocarriers. CAS micelles are spherical colloids of 50–500 nm in diameter and have an hydrophobic core formed by α_{s1}-casein, α_{s2}-casein, and β-casein, all of them bearing phosphoserine residues able to form strong ionic bonds with Ca^{2+} ions, and an hydrophilic shell of κ-casein as steric and electrostatic stabilizer.[21,22] According to these assembly properties, CAS micelles could be natural micellar nanocarriers for the transport of hydrophobic drugs to tumor tissue by passive targeting as well as for the internalization and controlled drug release.[20] Non-crosslinked micelles of CAS have previously been prepared for the entrapment, protection, and delivery of hydrophobic compounds such as curcumin,[23–25]

View Article Online
DOI: 10.1039/C8PY00600H

ergocalciferol (vitamin D2),[26] docosahexaenoic acid,[27] and meloxicam[28] among others. In addition, non-crosslinked CAS nanoparticles stabilized by lysine or arginine were recently designed for oral delivery of folic acid.[29] However, when non-covalently crosslinked micelles are used as drug carrier, the high dilution after injection in the bloodstream would lead to micelle dissociation and a premature drug release. To avoid the dissociation, the functionalities of CAS could provide anchoring points for the preparation of crosslinked structures using different chemical processes after micelle formation in order to obtain stable crosslinked casein micelles (CCM) that are suitable for systemic administration. In addition, the lack of a rigid, three-dimensional, and tertiary conformation of CAS causes it to be heat stable. Therefore it can be used in crosslinking processes at high temperatures.[21]

Different chemical routes have been evaluated for the preparation of crosslinked casein micelles (CCM), e.g., natural crosslinkers such as genipin and transglutaminase were used for the formation of stable CCM.[30–33] Moreover, sodium polyphosphate was used as ionic crosslinker of CAS micelles which were employed as carriers of flutamide for cancer therapy.[34] Despite several reports about the preparation of CCM, the employed crosslinkers in the literature did not introduce any stimuli−responsive properties to the micelles. In this sense, smart nanocarriers are considered as the new generation of materials in the field of controlled drug delivery.[35–38] Furthermore, the response of these CAS-based micelles to proteases, which are present in cells and overexpressed in various tumor types, has not been studied so far. The degradation by proteases could not only lead to a triggered release of the encapsulated drug in tumor cells overexpressing proteases but also assure the clearance of the carrier from the body after delivery of the cargo.

View Article Online
DOI: 10.1039/C8PY00600H

Here, we report the use of glyceraldehyde (GAL) as crosslinker of CAS micelles to produce pH-sensitive CCM. We hypothesized that the formation of imine groups (Schiff base) generated by the reaction with amine groups of CAS would give stable CCM at pH 7.4 but lead to hydrolysis at acidic pH. Combined with the enzymatic degradation, this could activate the release of hydrophobic drug molecules loaded into the micelles in a dual-responsive manner that can take place during the endocytic pathway. Thus, the crosslinker-induced pH-responsive property and the proteolytic degradability endow the CCM with dual-responsive release features that have not been studied so far. In this work, we report the preparation of smart CCM as carriers for hydrophobic drugs and the evaluation of their pH/protease dually responsive degradation and release behavior.

2. Experimental section

2.1. Materials

The following chemicals were used as purchased: Caseinate sodium salt (CAS, Sigma-Aldrich); DL-glyceraldehyde (GAL, Senn Chemicals); calcium chloride dihydrate ($CaCl_2.2H_2O$, Grüssing), sodium hydroxide (NaOH, Roth), sodium chloride (NaCl, VWR Chemicals), tri-sodium citrate dehydrate (TSC, Merck), urea (Sigma-Aldrich), acetic acid glacial (AA, Fisher Chemicals), sodium acetate (NaAc, Grüssing), sodium dihydrogen phosphate (NaH_2PO_4, Grüssing), disodium hydrogen phosphate (Na_2HPO_4, Grüssing), HPLC grade o-phthalaldehyde (OPA, Sigma-Aldrich), microscopy grade uranyl acetate 1 wt% solution (UAc, EMS), Nile red (NR, Sigma-Aldrich), deuterium oxide (D_2O, Sigma-Aldrich), and 3-(4,5-dimethylthiazol-2-yl)-2,5-diphenyltetrazolium bromide (MTT, Sigma-Aldrich).

View Article Online
DOI: 10.1039/C8PY00600H

2.2 Formation and characterization of CAS micelles

Casein micelles were reconstituted from CAS by dialysis of a protein solution (50 mg mL^{-1}) against a 0.05 mM $CaCl_2$ solution for 4, 6, 8, and 24 h using a dialysis membrane with molecular weight cut off (MWCO) of 10 kDa. After the dialysis process, re-assembled micelles were kept at 4 °C for 48 h and then centrifuged at 10,000 rpm for 10 min in order to precipitate protein aggregates. Finally, the hydrodynamic diameters of micelles were determined by dynamic light scattering (DLS) at 25 °C and 70 °C, which was chosen as the reaction temperature for crosslinking.

2.3 Synthesis of the CCM

In a typical procedure for the preparation of the CCM with different degrees of crosslinking, an aqueous dispersion of CAS micelles (10 mg/mL) and GAL was mixed to have a final crosslinker concentration of 1.8, 3.5, 7.0, or 14.0 mM. The reaction was carried out at 70 °C for 4 h under stirring conditions. Figure S1 in the Supporting Information (SI) shows a schematic illustration of the crosslinking mechanism between CAS amino groups and GAL. At the end of the reaction, the color of the dispersion changed from white to orange indicating that the protein crosslinking successfully occurred.[39] This change of color is due to the generation of chromophore as a consequence of the carbonyl-amine reaction from the ketoamine formed by the Amadori rearrangement as shown in Figure S1. The CCM were dialyzed against ultrapure water (4 changes of water) using a 50 kDa MWCO membrane. Finally, samples were kept at 4 °C prior to analysis.

2.4 Determination of the crosslinking efficiency – OPA method

The effective percentages of amine groups crosslinked with GAL were determined by a spectrophotometric assay using o-phthaldialdehyde (OPA) as fluorescent amino marker.

View Article Online
DOI: 10.1039/C8PY00600H

The OPA method exploits the reaction with primary amino groups of proteins to form highly fluorescent 1-alkylthio-2-alkyl–substituted isoindoles, which showed an absorption maximum at 340 nm.[40] This reaction was carried out in the presence of 2-mercaptoethanol, at pH 9.5, and at room temperature. For the analysis, 100 μL of CCM dispersion (1% w/w) were mixed with 2 mL of freshly prepared OPA reagent (80 mg of OPA in 2 mL absolute ethanol, 50 mL of 0.1 M sodium borate solution, pH 10, 5 mL of 20% SDS solution, and 0.2 mL of 2-mercaptoethanol filled to 100 mL with water). The absorbance was measured at 340 nm by UV-spectroscopy against OPA reagent as reference. The amino group concentration was determined on the basis of the measured absorbance and a calibration curve using glycine as standard (see Figure S2 of SI).

2.5 Size characterization and stability test

The hydrodynamic diameters (Z-average) of CCM were measured by DLS using a Zetasizer Nano ZS (Malvern Instruments). Measurements were carried out at a scattering angle of 173° and a laser wavelength of 633 nm. Dispersions (10 mg/mL) were previously diluted 1:10 in water, 10 mM phosphate buffer pH 7.4 with 0.14 M NaCl, or 10 mM acetate buffer pH 5 with 0.14 M NaCl, respectively, and measured by DLS at 25 and 37 °C. DLS was also used to study the resistance of CCM against dissociating agents. Dispersions were diluted 1:10 in 100 mM sodium citrate at pH 7.1, in 8 M urea at pH 9.3 or in 0.01 M NaOH at pH 12. Non-crosslinked micelles were used as control. Nanoparticle tracking analysis (NTA) was performed using a NanoSight NS500 equipment (Malvern). NTA measurements were carried out at 25 °C from water diluted samples (2×10^{-4} mg/mL, lower than the casein critical micellar concentration 0.1 mg/mL).

View Article Online
DOI: 10.1039/C8PY00600H

2.6 Characterization by TEM and SEM

The morphology of casein micelles was studied by means of transmission electron microscopy (TEM) using a Hitachi SU8030 microscope. To this effect, a drop of diluted dispersion (0.01 wt% of solids content) was placed on a carbon–coated copper grid. After drying, a drop of 1 wt% uranyl acetate (UAc) solution was added as a staining agent. Additionally, scanning electron microscopy (SEM, Zeiss Sigma) was used as a complementary technique in order to evaluate the nanocarriers morphology. CCM were coated with gold in a sputter coater and observed under an accelerating voltage of 2.0 kV.

2.7 Rheological characterization of the CCM

Rheology tests were performed on a Malvern Kinexus Pro rheometer in the frequency range of 0.1−100 Hz at 25 °C, using a 60 mm cone-plate geometry and sample concentration of 100 mg/mL. To ensure the rheological measurements within a linear viscoelastic region, a dynamic amplitude sweep was conducted prior to the frequency sweep, and the corresponding strain was determined to be 1%.

2.8 Degradation studies of the CCM by GPC

The degradation of the CCM in plasma or simulated lysosomal conditions was analyzed by gel permeation chromatography (GPC). Samples with a concentration of 1 mg/mL were incubated in 10 mM phosphate buffer pH 7.4, 10 mM acetate buffer pH 5 or 10 mM acetate buffer pH 5 plus trypsin (0.5% wt/wt) for 24 h at 37 °C. After incubation, samples were characterized by GPC using a Shimadzu Prominenze-i LC-2030 system equipped with a Shimadzu RID-20A refractive index detector. The GPC column used was a Shodex OHpak SB-806M HQ, with an OHpak SB-G 6B as a guard

View Article Online
DOI: 10.1039/C8PY00600H

column. Measurements were carried out in phosphate or acetate buffers at a flow rate of 1 mL/min.

2.9 Cytotoxicity of CCM

HeLa cells were obtained from the Leibnitz Institute DSMZ - German Collection of Microorganisms and Cell Cultures (#ACC 57). 10,000 cells per well were seeded into 96-well plates in 100 µl per well RPMI 1640 medium (Lonza) containing 10% fetal bovine serum (FBS Superior, Merck), 1% penicillin/streptomycin (Thermo Fisher Scientific) and 1% minimum essential medium (MEM) non-essential amino acids (Sigma-Aldrich) and grown at 37 °C and 5% CO_2 overnight. The next day, the medium was replaced with fresh medium containing various dilutions of test compound dispersions in duplicates and incubated for 48 h at 37 °C and 5% CO_2. The cell culture supernatant was removed and cells were washed twice with 200 µL/well phosphate buffer saline (PBS). Then, 100 µL/well fresh full medium and 10 µL/well MTT (Sigma-Aldrich, 5 mg/ml in PBS) were added and incubated for another 4 h at 37 °C. After development of formazan crystals, the cell culture supernatant was removed and crystals were dissolved by addition of 100 µL/well of isopropanol containing 0.04 M HCl. Absorbance was read at 590 nm in a Tecan infinite M200 Pro microplate reader. Relative viabilities were calculated by dividing average absorbance values of wells with treated cells by values of untreated cells (= 100% viability). All tests were repeated 3 times independently and errors were expressed as standard error of the mean (SEM).

2.10 Encapsulation of hydrophobic Nile red (NR)

For the encapsulation of NR into the micelles, 100 µL of dye solution (1 mg/mL) in methanol was transferred into a glass vial and methanol was evaporated to obtain a thin film. Then 4 mL of CCM solution (5 mg/mL) were added to the vial and stirred

View Article Online
DOI: 10.1039/C8PY00600H

overnight under exclusion of light. After removal of any free dye by centrifugation (3000 rpm for 2 min), the loaded dye was extracted from the micelles by diluting the samples with methanol and separation of precipitated micelles by centrifugation. NR content was quantified in the respective samples by UV-Vis spectrophotometry (λ = 552 nm) using a calibration curve of the NR measured in methanol. Encapsulation efficiency was defined as the weight percentage of the dye loaded versus the amount added to the micelles dispersion, and loading capacity was calculated as the weight percentage of dye relative to the micelles.

2.11 Release of NR from the CCM

For release studies of NR from the nanocarriers, 100 µL of loaded CCM (1 mg/mL) were incubated in phosphate buffer of pH 7.4 or acetate buffer of pH 5 containing trypsin (10 µL of 0.005% trypsin solution) at 37 °C in a 96-well plate. The assay was performed on a Tecan InfiniteM200 Pro microplate reader. Immediately after the start of the incubation, fluorescence intensity was recorded every 3 minutes at an excitation wavelength of 535 nm (9 nm bandwidth) and an emission wavelength of 612 nm (20 nm bandwidth). Average values from the duplicates were plotted against time.

2.12 Cellular uptake of CCM loaded with Nile Red

10,000 HeLa cells/ml were seeded onto cover slips in 24-well plates and grown over night in RPMI1640 (Lonza) 10% FBS (FBS Superior, Merck) 1% penicillin/streptomycin (Thermo Fisher Scientific) 1% MEM non-essential amino acid solution (Sigma-Aldrich) at 37 °C and 5% CO_2. The next day, the medium was replaced with fresh medium without supplements and without phenol red and micelles were added to a final concentration of 1 mg/mL. After 6 h of incubation at 37 °C, cells were washed 3 times with PBS and fixed with 10% neutral buffered formalin for 20 minutes

View Article Online
DOI: 10.1039/C8PY00600H

at room temperature. Then, objects were washed 3 times with PBS and stained with 4',6-diamidino-2-phenylindole (DAPI, 5 µg/mL in PBS, Sigma-Aldrich) for 30 minutes at room temperature. After another washing step, objects were mounted on microscope slides using ProTaqs Mount Fluor (Quartett GmbH) and dried overnight. Images were acquired with a Leica SP8 confocal laser scanning microscope using LASX software.

3. Results and Discussion

3.1 Controlled formation of casein micelles

Livney *et al.* have reported that CAS micelles could be re-assembled *in vitro* from a CAS solution, by adding tripotassium citrate, K_2HPO_4, and $CaCl_2$.[26,27] Following this procedure, they obtained micelles with diameters of around 147 nm. The average size in milk is 150 nm. However, micelle sizes could hardly be tailored by this methodology, which results in a disadvantage for the design of DDS. Moreover, the addition of Ca^{2+} in bulk could produce a premature aggregation of the CAS micelles and consequently increase the dispersity of the sample. Thus, in this work, a new and controlled process for the formation of CAS micelles was developed through the dialysis of CAS solution against 0.5 mM $CaCl_2$ for 4, 6, 8, and 24 h. The slow diffusion of Ca^{2+} through the dialysis membrane towards the casein solution allowed an adequate control over the formation of the CAS micelles, as shown schematically in Figure 1. The size distributions by intensity of the micelles formed after different dialysis times are depicted in Figure 2. Micelles showed a hydrodynamic diameter at 25 °C of 128.0 (PDI 0.228), 142.4 (PDI 0.241), 146.1 (PDI 0.222), and 509.1 nm (PDI 0.266) for 4, 6, 8, and 24 h of dialysis, respectively. In this way, micelle size could easily be tuned by controlling the time of dialysis as shown by increasing micelles sizes over time. The accumulation of Ca^{2+} by the diffusion-driven process probably caused aggregation of

View Article Online
DOI: 10.1039/C8PY00600H

the CAS micelles at some point, and consequently larger sizes were observed. Moreover, when the measurement temperature was increased until 70 °C micelle sizes increased up to 177.9 (PDI 0.086), 180.7 (PDI 0.131), 185.3 (PDI 0.126), and 879.5 nm (PDI 0.230) for 4, 6, 8, and 24 h, respectively. The increase in temperature may have produced a major uptake of water leading to a higher swelling of the micelles. Interestingly, the PDI of the micelles decreased at higher temperatures. Similar results were reported by Beliciu and Moraru,[41] where micelle size increases were attributed to the aggregation of κ-CAS. However, the reasons for the decrease in the PDI are still under investigation.

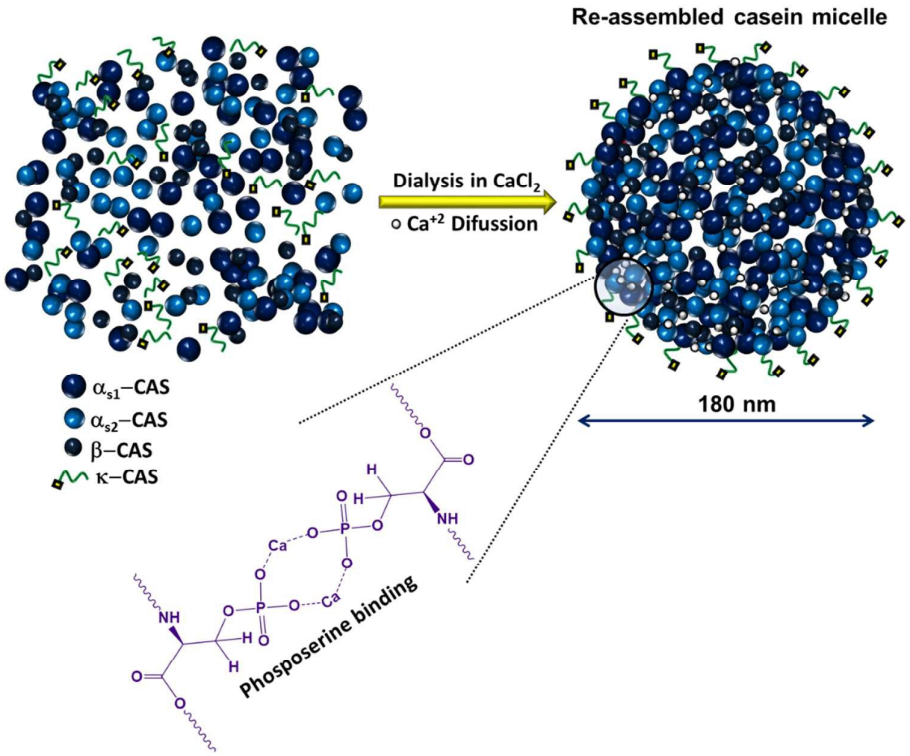

Figure 1. Schematic illustration of dialysis process for CAS micelle formation.

View Article Online
DOI: 10.1039/C8PY00600H

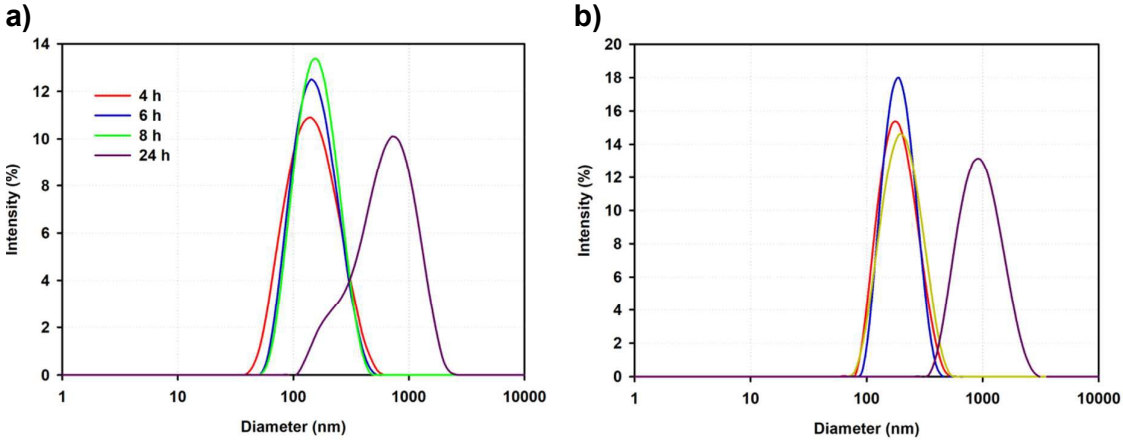

Figure 2. Size distributions by intensity of CAS micelles formed by dialysis against $CaCl_2$ at different times. Measurements at (a) 25 °C and (b) 70 °C.

According to the application requirements intended for these micelles as DDS in cancer therapy, dialysis for 4 h followed by crosslinking at 70 °C could be favorable conditions to produce stable nanocarriers with sizes below 200 nm and adequate PDI. It is widely accepted by the scientific community that nanoparticles with sizes between 50 and 200 nm are ideal for the application as carriers in cancer therapy.[42] It has been described that nanoparticles with sizes below 200 nm can evade the reticuloendothelial system (RES) after intravenous injection and consequently show longer circulation times *in vivo*.[42] In addition, nanoparticles with sizes lower than 5 nm are eliminated by renal clearance after injection in the bloodstream and nanoparticles between 5 and 50 nm can rapidly accumulate in the spleen.

3.2 Synthesis of the CCM

Although the micellar sizes suggest that they could be suitable as DDS, it is also known that non-crosslinked micelles are prone to suffer dissociation *in vivo* due to the dilution under these conditions, which consequently leads to premature release of the payload. Thus to increase the micelle stability, a crosslinking process was performed at 70 °C by addition of GAL to the prepared CAS micelles as shown in Figure 3.

View Article Online
DOI: 10.1039/C8PY00600H

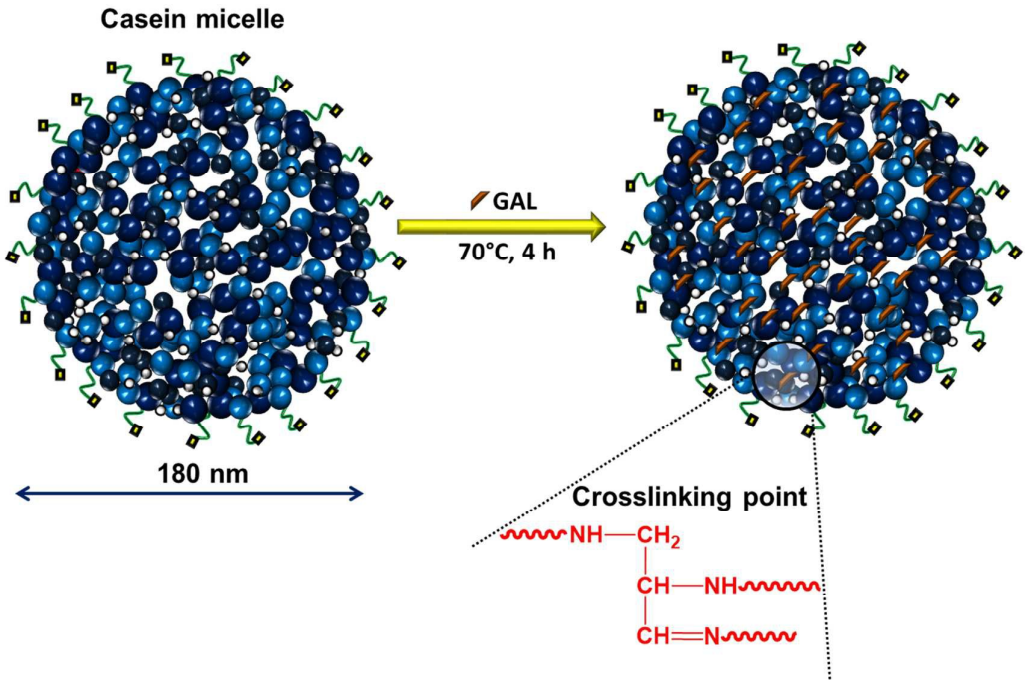

Figure 3. Schematic illustration of the crosslinking process used to obtain the CCM.

CCM were prepared with increasing GAL concentrations from 1.8 to 14 mM. The products were identified as $CCM_{1.8}$, $CCM_{3.5}$, CCM_{7}, and CCM_{14} according to the GAL molar concentration used in each reaction. With an increasing amount of crosslinker, a more intense orange color was observed in the products giving a visual indication that the crosslinking process successfully occurred (see Figure S3 of the SI). Although attempts to obtain spectroscopic evidences of the crosslinking reaction by ^{1}H-NMR and FTIR were made, the complexity of the CAS spectra obtained from both techniques did not allow inferring any clear conclusion on the crosslinking effectivity reached with GAL. However, as it will be demonstrated in the following sections, the crosslinking reaction could be confirmed by: i) the consumption of amine groups determined by the OPA method, and ii) experiments of structural stability of micelles performed by DLS.

View Article Online
DOI: 10.1039/C8PY00600H

3.3 Evaluation of the crosslinking efficiency

The degree of micelle crosslinking is a key parameter in the design of this kind of delivery agents, since it would allow a fine control over their degradation rate by proteases. The amount of CAS amine groups involved in the micelles crosslinking process was determined by a spectrophotometric method using OPA as amino marker. The crosslinking mechanism of proteins with GAL was previously proposed by Forni *et al.*,[43] as shown in Figure S1. Although this mechanism suggest that GAL would able to react with three amine groups from proteins, the crosslinking of three different CAS chains may be unlikely due to steric hindrance factors. Table 1 shows the number of remaining amine groups from lysine and arginine after crosslinking of the micelles. As it was expected, when the crosslinker amount was increased, more amine groups were consumed during the crosslinking process. In this way, when using a GAL concentration of 14 mM, 92% of the available amine groups were consumed. These results indicate that CCM_{14} presents the highest crosslinking density and therefore it could show superior structural stability and resistance to proteolytic degradation.

Table 1. Number of remaining lysyl and arginyl residues and crosslinking efficiency for CCM.

Product	Remaining NH_2/CAS molecule	Available NH_2 groups consumed
Non-CCM	50	-
$CCM_{1.8}$	24	48%
$CCM_{3.5}$	15	70%
CCM_7	10	80%
CCM_{14}	4	92%

View Article Online
DOI: 10.1039/C8PY00600H

3.4 Hydrodynamic diameter of the CCM by DLS

CCM sizes and stability under physiological salt concentrations and different pH conditions were determined by DLS. Here, we varied the pH values from pH 7.4 to pH 5 to simulate the conditions the CCM would face during the circulation and cellular internalization pathway. Table 2 shows the hydrodynamic diameters and the PDI of the CCM under physiological and endo-lysosomal conditions.

Table 2. Hydrodynamic diameters and PDI of the CCM at simulated physiological conditions.

Products	Mean diameter (PDI) in water at 25 °C [nm]	Mean diameter (PDI) pH 7.4 at 25 °C [nm]	Mean diameter (PDI) pH 7.4 at 37 °C [nm]	Mean diameter (PDI) pH 5 at 25 °C [nm]	Mean diameter (PDI) pH 5 at 37 °C [nm]
$CCM_{1.8}$	188.0 (0.137)	184.6 (0.119)	182.1 (0.145)	-[a]	-[a]
$CCM_{3.5}$	202.1 (0.246)	185.3 (0.120)	185.2 (0.122)	-[a]	-[a]
CCM_{7}	180.0 (0.150)	175.2 (0.132)	176.0 (0.111)	236.5 (0.152)	-[a]
CCM_{14}	181.8 (0.181)	170.5 (0.129)	172.8 (0.106)	157.8 (0.116)	158.1 (0.115)

[a] Unstable sample with aggregate formation.

All the CCM sizes presented at physiological conditions (pH 7.4 and 0.14 M NaCl at 37 °C) were between 172 and 185 nm with PDI minor to 0.200. Furthermore, Table 2 shows that micelle sizes were not significantly affected by the crosslinker concentration employed, which is in agreement with the results reported by Gaucheron *et al.*[31] for genipin crosslinked micelles. This result suggests that a rigid micellar structure can be obtained with low GAL amounts and further crosslinker addition further improves the micelle integrity (see Figure 4b) without important changes in their swelling capability. It can be noted that except for the highest GAL concentration, CCM were colloidally unstable at pH 5 and 37 °C. In these cases, micelle precipitation was induced by protein

View Article Online
DOI: 10.1039/C8PY00600H

aggregation as the pH value was close to the isoelectric point of CAS (pH 4.8). On the other hand, CCM_{14} was colloidally stable even at low pH probably due to the rigidity imposed by its higher crosslinking density. Despite $CCM_{1.8}$, $CCM_{3.5}$, and CCM_{7} samples were unstable at pH 5 and 37 °C, the aggregation of these systems inside the lysosomes may be unlikely, due to the low micelles concentration that would be achieved in the cells. The presence of proteases in those organelles (e.g. Cathepsin B), which are overexpressed in tumor cells, could degrade the CCM preventing protein aggregations. However, the size and stability under acidic conditions of CCM_{14} suggest that this carrier is the most promising for the utilization as DDS for cancer therapy.

3.5 Number size distribution of the CCM by NTA

In order to determine the micelle sizes at diluted conditions and confirm the crosslinked structure of the systems, we analyzed the micelles using NTA on water–diluted samples at 25 °C. All the CCM presented average sizes between 123 and 138 nm with narrow distributions as it is shown in Figure 4. In agreement with results obtained by DLS, a correlation between the crosslinking degree and the size in dispersion of the CCM was not observed. In addition, NTA confirmed the micellar crosslinking since they were stable in dispersion with concentrations hundred times below the critical micellar concentration of the CAS. At this point, it is worth to mention that non-crosslinked micelles were completely dissociated at the dilutions used for NTA measurements. In video 1 to 4 of the SI, the scattered light of the CCM was recorded in real time showing the Brownian motion of the particles. The analysis of the videos showed that the nanoparticles present sizes ranging from 90 to 230 nm, as was also determined by DLS, which could be suitable for cancer therapy applications.

View Article Online
DOI: 10.1039/C8PY00600H

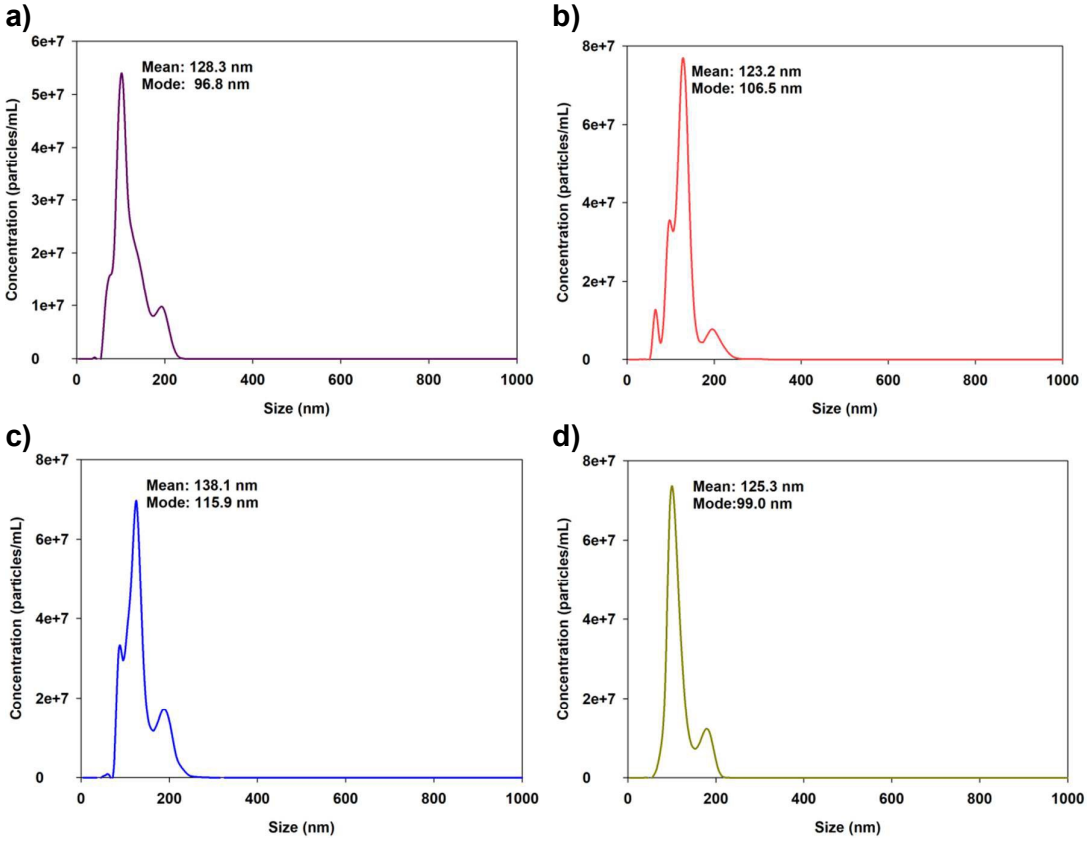

Figure 4. Size distributions of $CCM_{1.8}$ (a), $CCM_{3.5}$ (b), CCM_{7} (c) and CCM_{14} (d) as measured by NTA. Mode values are referred to the main peaks of the distributions.

3.6 Morphology of the CCM

Microscopy images of the CCM could give information about the morphology and dispersity of the samples. Thus, TEM images of the CCM were taken under vacuum. The images show that the CCM presented spherical morphology with acceptable size distribution, and no distinct differences were observed between systems with varied GAL concentration. An image of CCM_{14} is shown in Figure 5a as a representative example. The CCM particle size was around 160 nm in dry state in concordance with the results obtained by DLS and NTA. Moreover, small black dots were observed in TEM images, which may correspond to slightly crosslinked micelles that collapsed and lost their structural integrity under the high vacuum conditions used for TEM analysis. However, these tiny particles were not observed by SEM (Figure 5b), wherein high

View Article Online
DOI: 10.1039/C8PY00600H

levels of vacuum are also utilized, and therefore this TEM artifact could be due to the use of the staining agent, UAc. From SEM image of Figure 5b could also be observed a similar particle size distribution as TEM. In addition, magnification of an individual micelle is shown in the upper left corner of the figure.

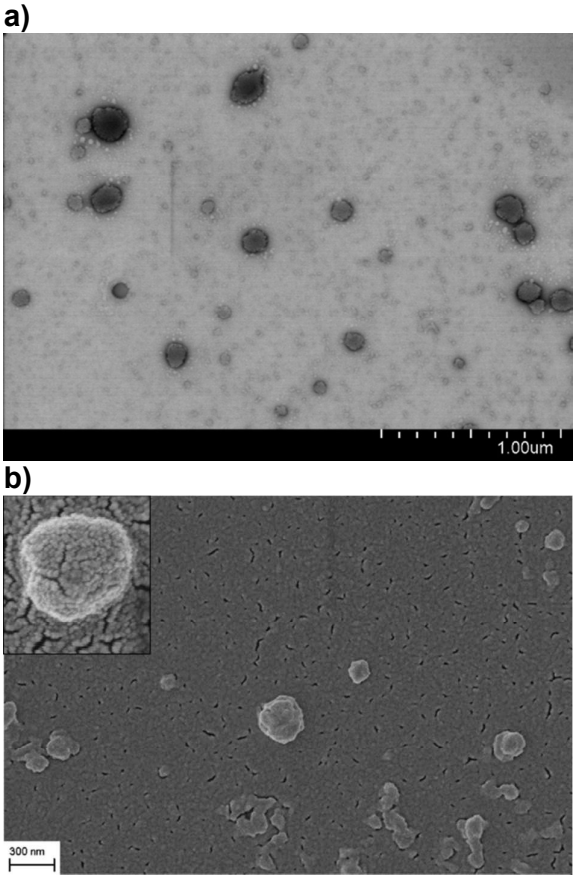

Figure 5. Morphology of CCM_{14} observed by TEM (a) and SEM (b).

3.7 Rheological behavior of CCM

Rheological tests over CCM gave information about the viscoelastic properties of the CCM to any applied force that allowed one to further prove their structural stability. Thus, the viscoelastic behavior of CCM dispersions was analyzed by rheological measurements with the aim to determine the effect of crosslinker concentration on the micellar structure. Measurements were performed at 25 °C with water dispersions of

View Article Online
DOI: 10.1039/C8PY00600H

CCM (100 mg/mL). Figure 6 shows frequency sweep experiments for different CCM at high concentrations. Clearly, it can be observed that the storage modulus (G') increased as the crosslinking degree of the CAS micelles was risen, from 4.91×10^{-3} Pa for $CCM_{1.8}$ to 1.089 Pa for CCM_{14} at 1 Hz. This result confirms that micelles stiffened with an increasing amount of crosslinking points in their structure. Regarding their applicability, crosslinking provided them a higher resistance to the shear stress present in the bloodstream. Our findings are in line with previous reports of interfacial dilational rheology for genipin-crosslinked micelles.[31]

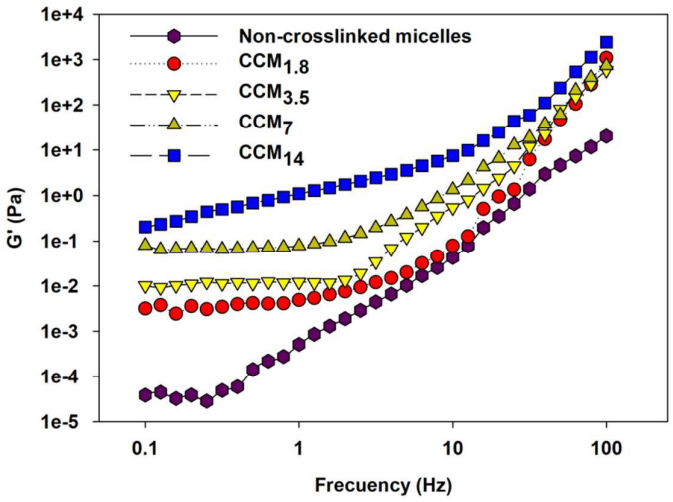

Figure 6. Storage modulus versus scanning frequency of non-crosslinked micelles and CCM at 25 °C.

3.8 Stability of the CCM

In order to measure the stability of CCM against micelle disrupting agents, the sizes of CCM were analyzed by DLS after the addition of urea and citrate, and in alkaline conditions. As reported earlier, non-crosslinked CAS micelles dissociate after the addition of urea due to the disruption of hydrogen bonding and hydrophobic interactions,[44] as well as when the colloidal calcium is solubilized by chelating agents (e.g., citrate or EDTA)[45] or under strong alkaline conditions (pH~12).[15] Figure 7a

View Article Online
DOI: 10.1039/C8PY00600H

shows the intensity-based size distribution of CCM_{14} before and after addition of urea, compared with non-crosslinked micelles. It could be observed that the use of urea as dissociating agent for the CCM resulted in particle swelling without destabilization of the colloidal integrity, which confirms the chemically crosslinked nature of the micelles. On the other hand, urea addition to non-crosslinked micelles led to a pronounced colloidal destabilization as it was evidenced by the notable broadening in the sample size distribution. The same tendency was observed for other dissociating agents such as sodium citrate and 0.01 M NaOH (pH 12) and it was depicted in Figure S4 of the SI. In these figures, it is possible to see that CCM sizes were not significantly affected by citrate chelation or alkaline conditions, while non-crosslinked CAS micelles resulted in colloidal unstable dispersions. It is worth mentioning that all remaining systems $CCM_{1.8}$, $CCM_{3.5}$, and CCM_7 were also stable against these dissociating agents (data not shown), which confirms their potential applicability as DDS. It was also observed that, regardless the dissociating agent used, micelles swelled to a minor extent as the crosslinker concentration increased, which indicated their higher structural integrity. In this case, the hydrodynamic sizes changed from 188 to 332 nm, from 202 to 301 nm, from 180 to 274 nm, and from 182 nm to 223 nm, for $CCM_{1.8}$, $CCM_{3.5}$, CCM_7, and CCM_{14}, respectively. This observation is in agreement with the results of crosslinking efficiency shown above. As an example, the size distributions that were obtained for urea as dissociating agent are shown in Figure 7b.

View Article Online
DOI: 10.1039/C8PY00600H

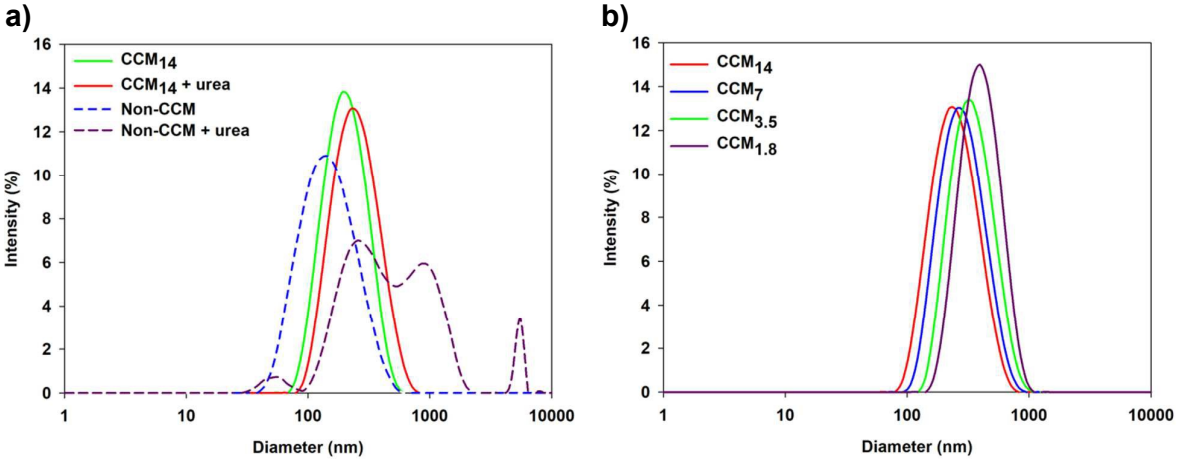

Figure 7. Size distribution by intensity of (a) CCM_{14} and non-crosslinked micelles and (b) all of the CCM systems after addition of urea as dissociating agent.

3.9 Degradation capability of the CCM under plasma and lysosomal simulated conditions

In order to study the degradation of CAS micelles in different pH conditions and in the presence of protease, CCM were analyzed by GPC after incubation in different degradation mediums. As it was previously mentioned, the presence of overexpressed proteases in cancer cells could activate the degradation of the CCM after cellular uptake and thus trigger a drug release process. Recently, Cohen *et al.*[46] assessed the *in vitro* digestive proteolysis of cholecalciferol (vitamin D3)–loaded non-crosslinked micelles. They showed that the non-crosslinked nanovehicles could be easily degraded by pepsin into small peptides (2–15 kDa), while the addition of trypsin led to the complete degradation of the casein. In this context, the question arises if the crosslinking could have any effect on the proteolytic degradation of the micelles. In addition, imine groups in the CCM could lead to destabilization of the micellar structure under acidic conditions. For this reason, degradation of CCM was evaluated by GPC at pH 5 in presence and absence of protease (trypsin was used as model protease) in order to simulate the lysosomal environment. Figure 8 shows the GPC chromatograms of CCM

View Article Online
DOI: 10.1039/C8PY00600H

samples after incubation for 24 h at 37 °C in different media. It can be observed that the chromatograms of samples incubated in PBS with pH 7.4 exhibited two peaks with elution times of around 11.3 min and 13.3 min, respectively. The signal at 11.3 min could be attributed to the CCM, while that of lower molecular weight (13.3 min) may have corresponded to the degradation products of micelles under these conditions. These results suggest that imine groups in the micelle structure could even be partly destabilized at pH 7.4. According to the chromatograms at pH 7.4, was also observed that the peak corresponding to the CCM decreased from CCM_{14} to $CCM_{1.8}$, while the peak of the degradation products increased. The crosslinking degree of these micelles showed a clear influence on the stability of the samples at pH 7.4. Therefore, when increasing the amount of crosslinker, the CCM became more stable under physiological conditions. On the other hand, under acidic conditions (pH 5), $CCM_{1.8}$, $CCM_{3.5}$, and CCM_{7} were completely degraded and only one signal was observed around 13.3 min. In the case of CCM_{14} with higher crosslinking density, a fraction of micelles remained after the incubation period, although in a minor proportion compared to pH 7.4. These results show that CCM could be suitable for degradation at simulated lysosomal pH, probably due to the hydrolysis of the imine groups formed in the crosslinking reaction. Moreover, after the addition of trypsin, all the samples including CCM_{14} were completely degraded. These results suggest that CCM_{14} would be the most stable system when circulating in the blood stream. At the site of the disease CCM_{14} could be completely degraded by the action of the lysosomal conditions (combination of acidic pH and presence of proteases). Thus, CCM_{14} seem to be the most promising candidate for its utilization as a carrier system for oncological drugs as it could maintain the cargo in plasma conditions (pH 7.4) but release the payload in intracellular conditions. For the other CCM, the major percentage of micelles already degraded at pH 7.4, which is

View Article Online
DOI: 10.1039/C8PY00600H

undesirable because the loaded drug could be prematurely released at plasma conditions before reaching the tumor. For this reason, CCM_{14} was chosen to explore the *in vitro* loading and release behavior with a model drug.

View Article Online
DOI: 10.1039/C8PY00600H

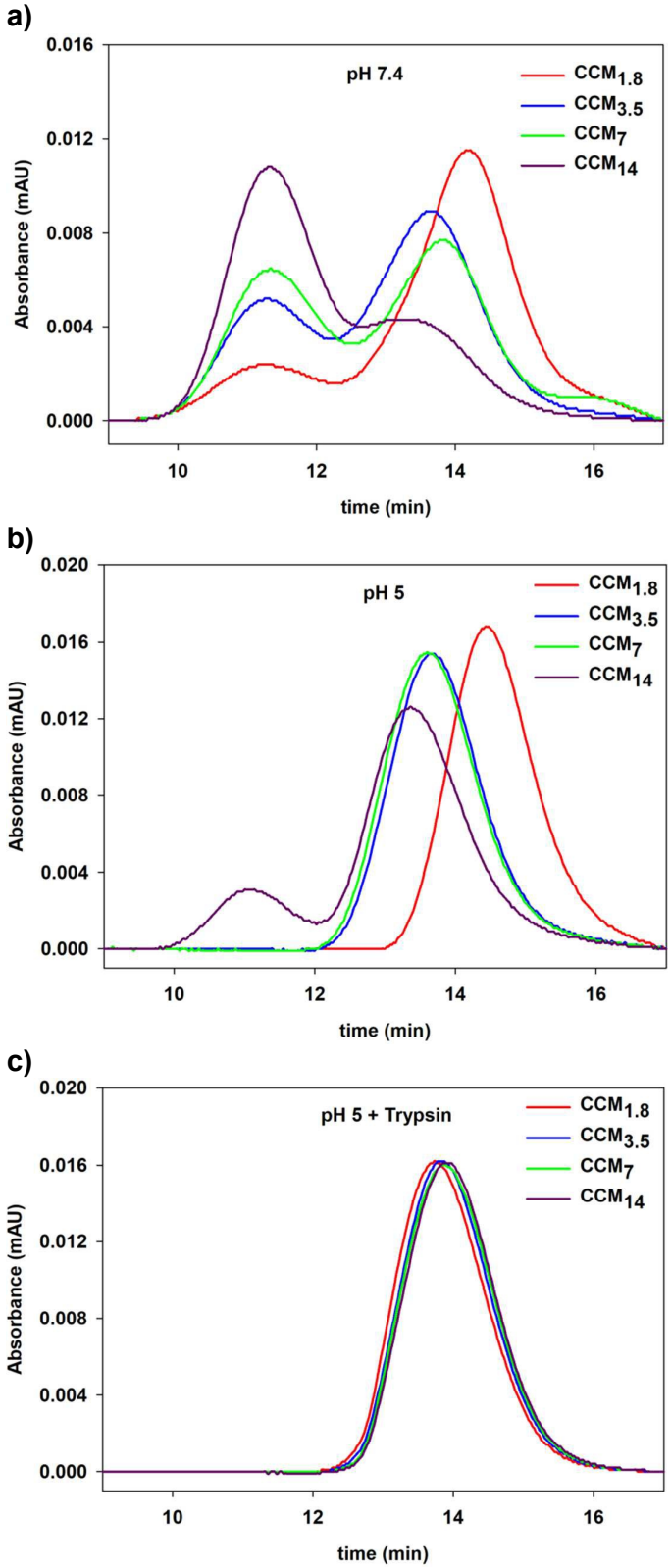

Figure 8. GPC chromatograms of CCM after incubation for 24 h at 37 °C in buffer pH 7.4 (a), pH 5 (b), and pH 5 plus trypsin (c).

View Article Online
DOI: 10.1039/C8PY00600H

3.10 Cytotoxicity of CCM

With the aim to show the potential use of CCM in cancer therapy, we investigated the effect of the carriers on the cell viability after 48 h in direct contact with cell culture. Figure 9 shows the resulting viabilities of cells after exposition to the different CCMs and non-crosslinked micelles as control. Up to a concentration of 10 µg/mL, all micelle dispersions tested caused a slight reduction of viability to around 70%, which is still considered to be non-toxic according to the norm ISO 10993-5. For the highest concentration of 1 mg/mL, preparations $CCM_{1.8}$ and $CCM_{3.5}$ caused a reduction in viability to about 50%, while CCM_7 and CCM_{14} were more toxic, which reduced the viability to about 30%. However, exposure to non-crosslinked micelles resulted in no further reduction of viability even at the highest tested concentration of 1 mg/mL. These results suggest that GAL was probably the source of toxicity of the nanocarriers. As mentioned above, it is expected that imine groups in the CCM structure are cleaved in acidic pH, and consequently some molecules of free GAL could be released into the cells. However, this fact does not compromise the use of the CCM in DDS, since they would never be applied in such high cytotoxic concentrations.

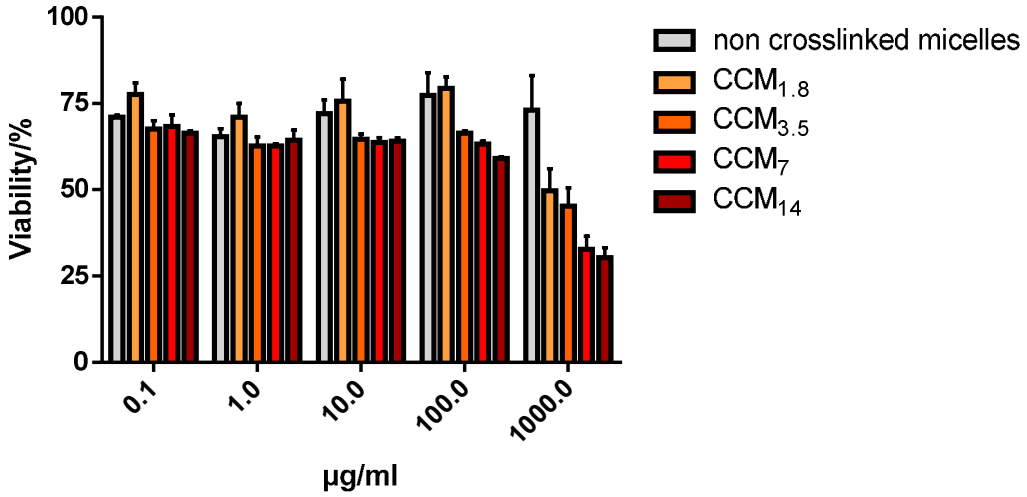

Figure 9. Dose–dependent viability of the CCM on HeLa cells.

View Article Online
DOI: 10.1039/C8PY00600H

3.11 Nile red encapsulation

The therapeutic application of poorly water−soluble drugs is a serious problem that the pharmaceutical industry is still struggling with. Even though many potent drugs were developed, they tend to fail due to their poor physico−chemical properties. With the objective of increasing the solubility of such candidates, we determined the capacity of the CCM to interact with highly hydrophobic drugs by testing the loading properties of CCM_{14} with NR as model compound. NR is a water−insoluble dye which could be solubilized in the hydrophobic core of CCM_{14}. For the dye encapsulation, the film method was employed where a thin film of NR was prepared by evaporation of a methanol solution. Then the CCM_{14} dispersion was added and stirred overnight. After removal of free NR by centrifugation, a notable increase in the "water−solubility" of NR was reached as is shown in Figure 10, indicating a good interaction between the CAS micelles and the dye. Indeed, CCM_{14} presented an acceptable loading capacity of 0.44% and an excellent encapsulation efficiency of 89% for the used dye/micelle ratio of 5 μg/mg. These results are comparable to the NR encapsulation in other DDS, e.g., in propylene sulfide–b–N,N-dimethylacrylamide micelles where 0.394% and 63.1% were reported for both parameters respectively, using a dye/polymer ratio of 6.25 μg/mg.[47]

View Article Online
DOI: 10.1039/C8PY00600H

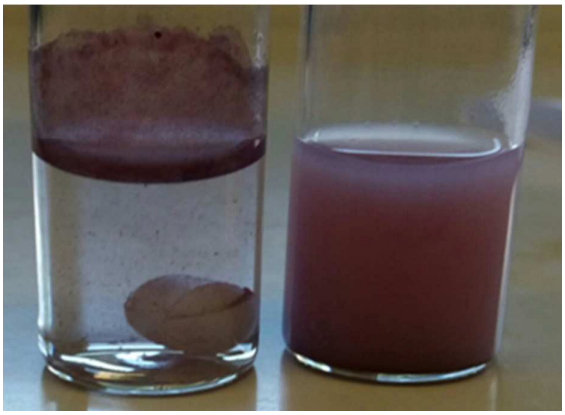

Figure 10. Dispersibility of the hydrophobic NR molecules after incubation in water (left) and with CCM_{14} (right).

3.12 Release of Nile red from the crosslinked micelles

For cancer therapy, it is highly desirable that the CCM can transport the drug under plasma conditions without premature release but, after reaching acidic conditions a triggered release should be activated for a therapeutic effect. For this reason, the release profiles of the NR–loaded CCM_{14} in different mediums, simulating plasma and lysosomal conditions were analyzed by following the dye fluorescence over time. Figure 11 shows: (a) the intensity of fluorescence as function over time and (b) the corresponding percentage of released dye in each medium used in the experiment. At pH 7.4, the fluorescence signal presented a small decay in the first minutes and then it increased to a constant plateau over time. This increase in fluorescence occurs due to the change in medium pH during the incubation (from slightly acidic in water to pH 7.4), which favors the hydrophobic interactions between the NR and the CAS micelles and thus achieving a better stabilization of the hydrophobic compound. According to this result, the dye is properly encapsulated and not released at pH 7.4 (Figure 11b). On the other hand, the intensity of the fluorescence signal showed a considerable and constant decay when the loaded CCM_{14} was incubated at pH 5 and in the presence of

View Article Online
DOI: 10.1039/C8PY00600H

trypsin. The observation can be explained by the degradation of the carrier in such conditions. The micelle disintegration produces a progressive release of NR towards the aqueous medium and, since NR is water–insoluble, it precipitates and decays in the fluorescence. Thus, a cumulative release of around 30% of NR was reached after 6 h. At this point, it is worth noting that despite the full disruption of the micellar structures after proteolytic cleavage as shown by GPC, a complete dye release was not achieved in the studied period of time. This behavior could be due to the formation of small protein particles, products of the degradation, which are able to entrap and stabilize the hydrophobic compound.[46] The presence of these protein particles was confirmed by following the hydrodynamic diameter of CCM_{14} during its incubation at pH 5 with trypsin for 24 h by DLS. The results are presented in Figure S5 of the SI, where after 12 h of incubation, the particle size of the degradation products was around 80 nm and remained constant until the end of the experiment. These results show the promising release properties of the CCM_{14} for their utilization as smart carriers, wherein they could maintain the cargo of the drug at physiological simulated conditions at pH 7.4 but enable the release of the cargo under lysosomal conditions at pH 5 and in the presence of proteases.

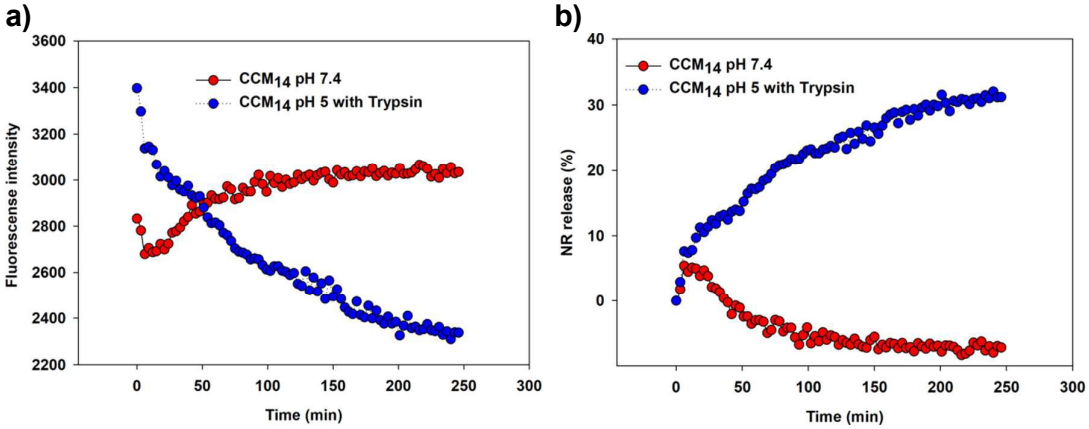

Figure 11. (a) Fluorescence intensity and (b) release percentage of NR over time at pH 7.4 (red) and at pH 5 with trypsin (blue).

View Article Online
DOI: 10.1039/C8PY00600H

3.13. Cellular uptake of CCM

For an efficient drug delivery the carrier needs to protect its cargo and transport it efficiently into the diseased cells where it can be released in a controlled way. Here, the delivery of NR into HeLa cells by CCM_{14} was assessed qualitatively by confocal laser scanning microscopy. NR fluorescence could clearly be detected in cells incubated with loaded CCM_{14} (Figure 12a) revealing the same staining pattern as cells treated with free NR (Figure 12b). As control, unloaded micelles were also incubated with cell to exclude background fluorescence from CCM (Figure 12c). Thus, NR was successfully delivered into the cells by means of CCM as a carrier. These results suggest that CCM can be internalized into HeLa cells and deliver their cargo in a controlled fashion as was demonstrated by *in vitro* release experiments.

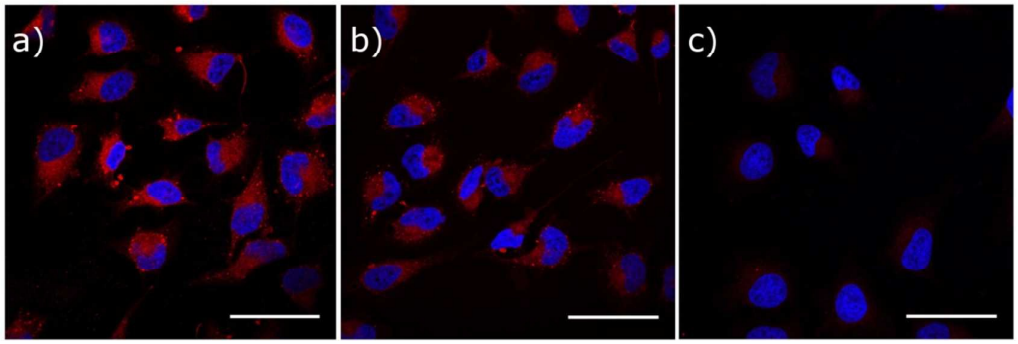

Figure 12. Delivery of NR as a hydrophobic model compound into cells. Confocal microscopy images of HeLa cells incubated with (a) CCM_{14} loaded with NR, (b) free NR (0.3μg/mL), and (c) unloaded micelles background control. NR fluorescence shown in red, nuclei were stained with DAPI (blue). Scale bar = 50 μm.

4. Conclusions

CAS micelles were prepared using a novel method based on the properties of the protein to form micelles in presence of Ca^{2+} ions, using a membrane for slow Ca^{2+}

View Article Online
DOI: 10.1039/C8PY00600H

diffusion. The CAS micelles were chemically stabilized by the addition of glyceraldehyde as crosslinker–forming imine bonds with the available amine groups of the protein. While the formulation with the highest crosslinker concentration (CCM_{14}) could be degraded at acidic pH and by proteases (similar to lysosomal conditions), they maintained their structure in simulated plasma conditions (PBS, pH 7.4). The hydrophobic dye NR could be successfully stabilized in the hydrophobic core of CCM_{14} with excellent encapsulation efficiencies. Moreover, the release of NR from CCM_{14} was negligible in plasma conditions but was highly accelerated at intracellular conditions (pH 5 and the presence of proteases). Finally, CCM showed no major toxicity when directly exposed to HeLa cells for concentrations up to 100µg/ml and could successfully deliver the encapsulated hydrophobic model drug NR into the cells. For this reason, we concluded that the as-prepared CCM are promising candidates for the application as carrier systems for the transport of oncological and hydrophobic drugs (e.g., doxorubicin, paclitaxel or docetaxel). According to the nanometric sizes and physicochemical properties analyzed here, we expect in an *in vivo* scenario that the particles accumulate in tumor tissue by the enhanced permeability and retention effect (EPR) and release the cargo only in intracellular compartments responding to enzymatic and pH changes.

Conflicts of interest

There are no conflicts to declare.

Acknowledgements

The authors gratefully thank UTN Villa Maria, UNC, UNL, ANPCyT, and CONICET, for financial support. Prof. Dr. M. Calderón gratefully acknowledges financial support from the Bundesministerium für Bildung und Forschung (BMBF) through the

View Article Online
DOI: 10.1039/C8PY00600H

NanoMatFutur award (13N12561), the Freie Universität Focus Area Nanoscale, and the Deutsche Forschungsgemeinschaft (DFG) through the Collaborative Research Center 1112, project A04.

Notes and references

1 H. Chen, Y. Chen, H. Yang, W. Xu, M. Zhang, Y. Ma, S. Achilefu and Y. Gu, *Polym. Chem.*, 2014, **5**, 4734.

2 C. Thiele, D. Auerbach, G. Jung, L. Qiong, M. Schneider and G. Wenz, *Polym. Chem.*, 2011, **2**, 209–215.

3 K. Bauri, M. Nandi and P. De, *Polym. Chem.*, , DOI:10.1039/C7PY02014G.

4 J. Xu, Z. Fan, L. Duan and G. Gao, *Polym. Chem.*, , DOI:10.1039/C8PY00319J.

5 H. K. and S. A. Shojaosadati, *Curr. Pharm. Des.*, 2016, 22, 3455–3465.

6 W. Lohcharoenkal, L. Wang, Y. C. Chen and Y. Rojanasakul, *Biomed Res. Int.*, 2014, **2014**, 4.

7 H. Kouchakzadeh and S. Abbas Shojaosadati, *Curr. Pharm. Des.*, 2016, **22**, 3455–65.

8 A. MaHam, Z. Tang, H. Wu, J. Wang and Y. Lin, *Small*, 2009, **5**, 1706–1721.

9 L. Yin, C. Yuvienco and J. K. Montclare, *Biomaterials*, 2017, **134**, 91–116.

10 A. O. Elzoghby, W. M. Samy and N. A. Elgindy, *J. Control. Release*, 2012, **161**, 38–49.

11 A. O. Elzoghby, W. M. Samy and N. A. Elgindy, *Pharm. Res.*, 2013, **30**, 512–522.

12 M. A. Gauthier and H.-A. Klok, *Polym. Chem.*, 2010, **1**, 1352.

13 G. Yaşayan, A. O. Saeed, F. Fernández-Trillo, S. Allen, M. C. Davies, A. Jangher, A. Paul, K. J. Thurecht, S. M. King, R. Schweins, P. C. Griffiths, J. P. Magnusson and C. Alexander, *Polym. Chem.*, 2011, **2**, 1567.

14 K. A. Gawde, P. Kesharwani, S. Sau, F. H. Sarkar, S. Padhye, S. K. Kashaw and A. K. Iyer, *J. Colloid Interface Sci.*, 2017, **496**, 290–299.

15 B. Vaia, M. A. Smiddy, A. L. Kelly and T. Huppertz, *J. Agric. Food Chem.*, 2006, **54**, 8288–8293.

16 M. B. Caspersen, M. Kuhlmann, K. Nicholls, M. J. Saxton, B. Andersen, K. Bunting, J. Cameron and K. A. Howard, *Ther. Deliv.*, 2017, **8**, 511–519.

17 L. Trynda-Lemiesz, *Bioorg. Med. Chem.*, 2004, **12**, 3269–3275.

View Article Online
DOI: 10.1039/C8PY00600H

18 Y. Boonsongrit, A. Mitrevej and B. W. Mueller, *Eur. J. Pharm. Biopharm.*, 2006, **62**, 267–274.

19 M. L. Picchio, A. J. Paredes, S. D. Palma, M. C. G. Passeggi, L. M. Gugliotta, R. J. Minari and C. I. A. Igarzabal, *Colloids Surfaces A Physicochem. Eng. Asp.*, 2018, **541**, 1–9.

20 A. O. Elzoghby, W. S. Abo El-Fotoh and N. a. Elgindy, *J. Control. Release*, 2011, **153**, 206–216.

21 D. J. McMahon and B. S. Oommen, *J. Dairy Sci.*, 2008, **91**, 1709–1721.

22 D. J. McMahon and B. S. Oommen, in *Advanced Dairy Chemistry: Volume 1A: Proteins: Basic Aspects, 4th Edition*, 2013, pp. 185–209.

23 A. Sahu, N. Kasoju and U. Bora, *Biomacromolecules*, 2008, **9**, 2905–2912.

24 M. Esmaili, S. M. Ghaffari, Z. Moosavi-Movahedi, M. S. Atri, A. Sharifizadeh, M. Farhadi, R. Yousefi, J. M. Chobert, T. Haertlé and A. A. Moosavi-Movahedi, *LWT - Food Sci. Technol.*, 2011, **44**, 2166–2172.

25 K. Pan, Y. Luo, Y. Gan, S. J. Baek and Q. Zhong, *Soft Matter*, 2014, **10**, 6820.

26 E. Semo, E. Kesselman, D. Danino and Y. D. Livney, *Food Hydrocoll.*, 2007, **21**, 936–942.

27 P. Zimet, D. Rosenberg and Y. D. Livney, *Food Hydrocoll.*, 2011, **25**, 1270–1276.

28 M. Cheema, A. N. Hristov and F. M. Harte, *J. Dairy Sci.*, 2017, 1–10.

29 R. Penalva, I. Esparza, M. Agüeros, C. J. Gonzalez-Navarro, C. Gonzalez-Ferrero and J. M. Irache, *Food Hydrocoll.*, 2015, **44**, 399–406.

30 T. Huppertz and C. G. de Kruif, *Int. Dairy J.*, 2008, **18**, 556–565.

31 N. F. N. Silva, A. Saint-Jalmes, A. F. de Carvalho and F. Gaucheron, *Langmuir*, 2014, **30**, 10167–10175.

32 X. Zhen, X. Wang, C. Xie, W. Wu and X. Jiang, *Biomaterials*, 2013, **34**, 1372–1382.

33 T. Huppertz, M. a. Smiddy and C. G. de Kruif, *Biomacromolecules*, 2007, **8**, 1300–1305.

34 A. O. Elzoghby, M. W. Helmy, W. M. Samy and N. A. Elgindy, *Int. J. Nanomedicine*, 2013, **8**, 1721–1732.

35 M. Giulbudagian, M. Asadian-Birjand, D. Steinhilber, K. Achazi, M. Molina and M. Calderón, *Polym. Chem.*, 2014, **5**, 6909–6913.

36 A. S. Sonzogni, M. C. G. Passeggi, S. Wedepohl, M. Calderón, L. M. Gugliotta, V. D. G. Gonzalez and R. J. Minari, *Polym. Chem.*, , DOI:10.1039/c7py01798g.

37 M. Asadian-Birjand, J. Bergueiro, F. Rancan, J. C. Cuggino, R.-C. Mutihac, K.

View Article Online
DOI: 10.1039/C8PY00600H

Achazi, J. Dernedde, U. Blume-Peytayi, A. Vogt and M. Calderón, *Polym. Chem.*, 2015, **6**, 5827–5831.

38 M. Wei, Y. Gao, X. Li and M. J. Serpe, *Polym. Chem.*, 2017, **8**, 127–143.

39 A. S. Acharya, Y. J. Cho and B. N. Manjula, *Biochemistry*, 1988, **27**, 4522–4529.

40 V.-J. K. Švedas, I. J. Galaev, I. L. Borisov and I. V Berezin, *Anal. Biochem.*, 1980, **101**, 188–195.

41 C. M. Beliciu and C. I. Moraru, *J. Dairy Sci.*, 2009, **92**, 1829–1839.

42 T. Sun, Y. S. Zhang, B. Pang, D. C. Hyun, M. Yang and Y. Xia, *Angew. Chemie Int. Ed.*, 2014, **53**, n/a-n/a.

43 F. Forni, R. Cameroni, G. Furiosi and G. Pifferi, Biodegradable microbeads for the pharmaceutical and cosmetic uses, Italian patent application,1993.

44 T. C. A. McGann and P. F. Fox, *J. Dairy Res.*, 1974, **41**, 45–53.

45 A. Pitkowski, T. Nicolai and D. Durand, *Biomacromolecules*, 2008, **9**, 369–375.

46 Y. Cohen, M. Levi, U. Lesmes, M. Margier, E. Reboul and Y. D. Livney, *Food Funct.*, 2017, **8**, 2133–2141.

47 M. K. Gupta, T. A. Meyer, C. E. Nelson and C. L. Duvall, *J. Control. Release*, 2012, **162**, 591–598.

View Article Online
DOI: 10.1039/C8PY00600H

Table of Contents Entry

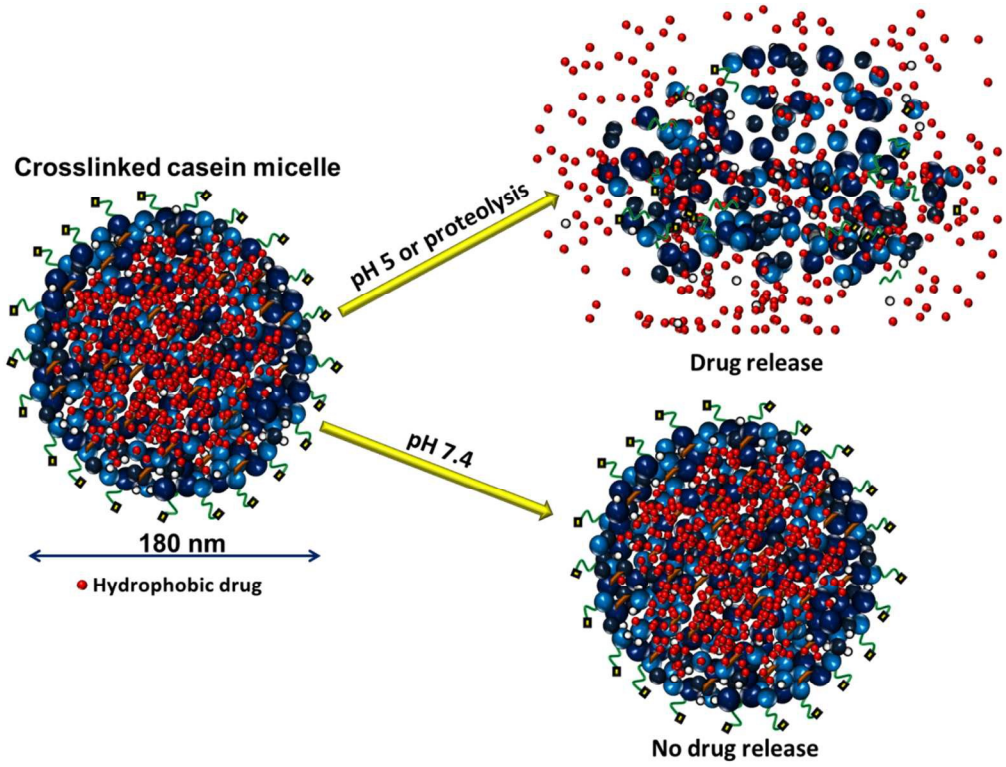

Crosslinked casein micelles with a dually pH and protease drug triggered release can be applied as a promising hydrophobic drug carrier material.